Design, Development, and Evaluation of a PV_Bio-Gen Range Extender for an Off- Road Electric Vehicle

Amin Ghobadpour*(**), Hossein Mousazadeh**‡, Sousso Kelouwani*,
Ahmad Sharifi Malvajerdi***, Shahin Rafiee**

* Université du Québec à Trois-Rivières, Trois-Rivières (Québec) G9A 5H7, Canada

** Department of Mechanical Engineering of Biosystems, University of Tehran, Karaj, Iran

*** Agricultural Engineering Research Institute, Agricultural Research, Education and Extension Organization, Karaj, Iran

(amin.ghobadpour@uqtr.ca, hmousazade@ut.ac.ir)

‡ Corresponding Author; Hossein Mousazadeh, Department of Mechanical Engineering of Biosystems, Karaj, Iran, Tel: +98 912 026 4801, Fax: +98 26 328 01011, hmousazade@ut.ac.ir

Received: 15.01.2020 Accepted: 10.03.2020

Abstract- Transformation from fossil fuels to clean energy is necessary due to the stricter environmental protection policies. Drivetrain hybridization by green energy sources seems to be an appropriate solution in farm applications. However, some constraints are raised, e.g., the low energy density of renewable energy sources and the long recharging time of batteries. Hence, the objective of this work is to suggest an Extended-Range Solar Assist Plug-In Hybrid Electric Tractor (E-RSAPHT) via a combination of a photovoltaic (PV) system and a biogas fuelled engine generator set (Bio-Gen) with a battery pack. Due to multi-power sources, a heuristic control strategy is proposed to split the generated powers while considering the extend daily operation hours. Moreover, some field measurements are conducted to define typical working cycles for farm hybrid vehicle application. Considering these points, the modelling, simulation and development of the E-RSAPHT are presented in this paper. Experimental results showed that the proposed system could improve energy autonomy and fuel efficiency. For typically evaluated toolbars, the operation ranges of the trailer, boom-type sprayer, and water-pump system were extended up to 292, 255, and 320% compared to the base battery-electric tractor, respectively. The conducted investigations illustrate that even for a 2100kg electric farm vehicle, a downsized 4.4kW Bio-Gen allows the hybrid-electric system to supply the power demand compared to the conventional system by using the internal combustion engine.

Keywords Hybrid Electric Tractor, Working cycle, Photovoltaic, Biogas fuelled engine generator.

List of Abbreviations

Bio-Gen	Biogas fuelled Engine Generator Set	GPS	Global Positioning System
CB	Charge Blended	HEV	Hybrid Electric Vehicle
CD	Charge Depletion	ICE	Internal Combustion Engine
CS	Charge Sustaining	NEDC	New European Driving Cycle
EMS	Energy Management System	PHEV	Plug-in Hybrid Electric Vehicle
E-REV	Extended-range Electric Vehicle	PTO	Power Take-Off
E- RSAPHT	Extended-Range Solar Assist Plug-in Hybrid Electric Tractor	PV	Photovoltaic
ESS	Energy Storage System	RE	Range Extender
EV	Electric Vehicle	SOC	State of Charge

1. Introduction

Since the main environmental problems are associated with the burning of fossil fuels, the vehicle industry has been in a period of energy transformation from fossil fuels to clean energy [1, 2]. Stricter environmental protection policies, such as European Stage V non-road emission standards [3], tightens the emission level in vehicles such as tractors. In this regards, drivetrain electrification and renewable energy applications seem to be alternative ways in the progress of agriculture 4th revolution, smart farming and farm energy independency [4, 5]. However, limited infrastructure, poor durability and long recharging time of the current batteries are some drawbacks of electrified powertrain in agriculture. These limitations would be more drastic in farm vehicles, which require more energy in a short time [6]. In automotive industry, various types of configuration, such as hybrid electric vehicles (HEVs) and fuel cell vehicles, have been proposed as a solution having the advantages of long mileage, low refuelling time, and flexible operating modes. However, the internal combustion engine (ICE) is the most common RE for HEVs to meet the power requirements of the driving load. Instead, in off-road vehicles, including the agricultural tractors, the powertrain hybridization is still at an initial stage. The HEVs driveline is usually categorized in two main architectures including Parallel and Series. In a parallel hybrid, the ICE and electric motor are coupled with transmission via the same drive shaft to propel the vehicle. In a series hybrid, the RE coupled with a generator to produce electricity. Actually, it is an ICE assisted electric vehicle (EV). Some advantages of series hybrid drivetrains are: a) mechanical decoupling between the engine generator and the driven wheels that allow a downsized ICE operate at its optimal region independently from the driver's request to meet some specific performance, economy, or emission targets; b) nearly ideal torque-speed characteristics of the electric motor make multi-gear transmission unnecessary [7]. Moreover, considering a bulky engine generator in a series hybrid, it is more suitable in traction and heavy applications like tractors. That is because there is usually enough space thus mass reduction is not an important objective for a tractor and could even seem like an advantage regarding the stability of the vehicle. A plug-in hybrid electric vehicle (PHEV) could be more suitable configuration for reducing fuel consumption because it might be charged with external electric power sources like a renewable power plant. However, due to multi-power sources of hybrid configuration, an appropriate EMS is necessary for efficient power splitting [1].

1.1. Specific Features of Agricultural Electric Vehicles from Working Cycles to On-Farm Energy Production

The criteria for designing a drivetrain for Off-Road vehicles is different from that of an automobile. As an illustration, tractors are usually designed for attaching different implements for transportation and field operating. They are conceived essentially with more weight to operate at lower speed and range of acceleration. Moreover, some filed tasks require extra power that could be provided by the Power Take-Off (PTO), hydraulic systems, and an electric outlet of the tractor.

In order to mitigate HEVs challenges, research in agricultural technologies is slanted towards alternative fuels and low-pollution energy systems such as biofuels and hybrid electric drivers. Tritschler et *al.* (2010) investigated the potential of a fuel cell hybrid drive train for agricultural tractors. The results showed that fuel cell systems still suffer from certain drawbacks, including a limited lifetime, high cost, hydrogen storage, and distribution infrastructure [8]. Xie et *al.* (2013) studied the design process of a medium-sized hybrid electric tractor. Their results showed that a hybrid electric tractor can improve about 19% of fuel economy compared to traditional tractors [9]. Gonzalez et *al.* (2016) developed an unmanned ground vehicle hybrid-powered robotic tractor. They mentioned that the new technologies built on clean energy sources could significantly reduce emissions of air pollutants and greenhouse gases. This occurred with the offloading of ICE and the addition of this load to an Electrical Storage System (ESS). This technique allows small farm tractors to move bigger implements, which have their own motors by the addition of an ESS [10, 11]. However, developing in the electrification of the agricultural vehicles seems necessary as a prerequisite for the smart farm.

In terms of performance assessment, conventional tractors are usually tested in specific conditions by different types of dynamometers. Nevertheless, the working cycle evaluation of tractors with different types of implements is time-consuming and costly [12]. In the automobile development process, some standard driving cycles are employed for the standard exhaust emission tests, component size and evaluate different technologies by use of simulators [1, 13]. A driving cycle indicates how vehicles are driven and is usually represented by a set of data points of vehicle speed versus time to computation of power demand based on vehicle parameters [14]. Nevertheless, due to differences in speed and application, most commonly driving cycles used in urban vehicles are not applicable directly in off-road vehicles such as tractors. However, some modern agricultural tractor manufacturers have evaluated their vehicles on a chassis dynamometer using the New European Driving Cycle (NEDC) [15], as well as scaled down (reduced in velocity) Urban Dynamometer Driving Schedule (UDDS) used for the evaluation of a low-speed vehicle [16]. However, it should be noted that in off-road applications, due to fluctuation in environmental conditions in terms of surface topography and soil deflection, the use of speed profiles lonely could not be adequate. Therefore, one of the purposes of this work is to derive some realistic typical "working cycles" in agricultural tractor applications to employ it in the hybrid electric tractor design process. In fact, the "working cycle" expression comes from the importance of considering the energy consumption rather than the speed profile in such applications like tractors with lower speed and higher torque.

Unlike urban vehicles, agricultural vehicles usually operate far from the electrical network and fuel stations. Therefore, providing energy to these areas increases the cost of farming. In this case, an independent on-site renewable power supply system can provide a meaningful alternative while helping to meet the farm energy demand or sell electricity to the local network [5, 17]. In addition, this could help to improve efficiency and reduce dependency on fossil

fuels, as well as providing distributed electricity generation [18]. The sun and biomass are the most available energy sources in the farm. These types of energies might be converted to electricity or heat. Furthermore, the biomass could be used to produce other types of fuels such as biogas, bioethanol, and biodiesel [19]. The biogas produces via the anaerobic digestion of crops and wastes. Raw biogas is roughly 60% bio-methane and 35% CO2 with trace elements of H2S. It is not high quality enough to be used as fuel gas for vehicles. The solution is the use of biogas upgrading or purification processes. The bio-methane content of standard upgraded Biogas (type A) is more than 97% [20] that could be used as green fuel in gas-fuelled engines.

Consequently, the main objective of this research is to define typical working cycles, based on experimental test, in order to develop a renewable energy based hybrid electric off-road vehicle as a multipurpose farm tractor. Besides, on-farm renewable energy sources including photovoltaic (PV) and biogas are used as recharging source options. Moreover, because there is no standard method for component sizing and evaluation method for hybrid electric tractor platform in agricultural application, an appropriate energy model should be worthwhile for tuning the EMS and components sizing by employing the working cycle before the implementation in a real platform. The rest of this paper proceeds as follows. The project background, modelling, developing method, and EMS are described in section 2. In section 3, EMS experimental setup and real-word test definition to derive working cycles with the developed vehicle are described; section 4 presents simulation results and their validation by empirical data. Finally, conclusions are drawn in section 5.

2. Materials and Methods

2.1. Project Background and Developing Method

In this research, an existing Solar Assist Plug-in Hybrid electric Tractor (SAPHT) [21] is developed as a renewable energy based series Extended- Range Solar Assist Plug-In Hybrid Electric Tractor (E-RSAPHT). The SAPHT was a pure electric, low-speed Off-Road vehicle designed for agricultural light applications. Speed range was limited up to 25 km/h and the power range was 0 to 35 kW. The powertrain system consists of three electric motors (two for driving wheels and one for the PTO and lifting systems) with single-speed gearboxes. Two different sources of electrical energy were supplied to the SAPHT: on-board PV arrays and grid electricity. A 16.8 kWh lead-acid battery pack is utilized as ESS to supply energy. Although the regenerative braking system's functionality existed in the basic SAPHT, it was ignored due to design constraints and low speed. Despite acceptable energy efficiency in SAPHT, because of the limitations of the EVs, it was faced with lack of energy in various operations [21] that it occurred due to the fast degradation of the battery.

As aforementioned, series hybrid architecture is more suitable in traction and heavy applications such as tractors. Therefore, the SAPHT was developed to become the series E-RSAPHT as shown in Fig.1. The new power sources include the on-board PV system, Bio-Gen, and ESS. The model-based design is used as a powerful engineering aid tool to simulate vehicles in a computer before construction. Nevertheless, models always have some limitations due to assumptions. The E-RSAPHT modelling process is described in the following sections.

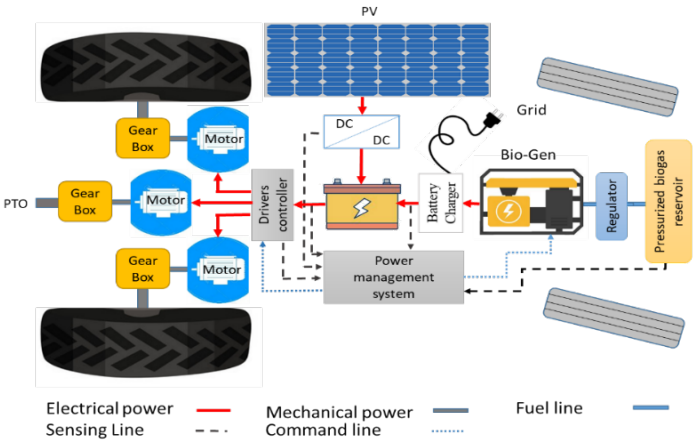

Fig. 1. Simplified E-RSAPHT project schematic diagram.

2.2. Powertrain Model

The vehicle subsystems are modelled in detail in the author's previous work [21]; therefore, it would not be repeated here. However, a new hybrid architecture is built in this research in order to include the RE and EMS. We will only mention some fundamental aspects that are necessary to develop the E-RSAPHT powertrain.

Besides, an overall MATLAB Simulink model was developed to simulate the E-RSAPHT as shown in Appendix A. This simulation tool provided a basis for sizing individual components such as RE by estimating the total energy requirement for working cycles and working time. In addition, it can be used for implementing various EMS control strategies prior to practical experiments. In order to increase the simulation speed time, for components including the battery, PV system, Bio-Gen, and electric machines, a lookup table data and efficiency map was considered that was provided by the manufacturers and experimental test results. The main components parameters and specifications of the E-RSAPHT from authors' previous research work [21] are listed in the Table 1, which were used in the model. The methodology for the modelling of main components are detailed in the following sections.

2.3. Agricultural Tractor Model

A typical agricultural tractor dynamic movement is generally modelled as a dynamic point mass (mass of the vehicle and the equivalent mass of the rotating parts) that can move forward by exerting propulsion power. To overcome the resistive force (F_{res}) of the SAPHT and its attached implements the following equations are determined [21]:

$$M_{tot.}\frac{d}{dt}v_{ev} = F_{tr} - F_{res} \quad (1)$$

$$F_{res} = F_{roll} + F_{air} + F_{acc} + F_{hill} + F_{drawbar} \quad (2)$$

Table 1. The main components parameters [21].

Parameter	Symbol	Value
Gear ratio efficiency	η_g	90%
Gear ratio	G	18.66
Battery cycle efficiency	$\eta_{Bat.}$	83%
Front area	A	1.8 m^2
Aerodynamic drag coefficient	C_d	0.2 to 0.4
Rolling resistance coefficient	C_{roll}	
Asphalt		0.029
Sand road		0.03 to 0.05
No-tilled field		0.04 to 0.065
Tilled field (harrow and		0.09 to 0.16
Drive tire radius	r	0.55 m
Air density	ρ	1.25 kg m^{-3}
Gravity acceleration	g	9.80 m/s^2
SAPHT total mass	m	2100 kg
Moment of inertia for motor's	I	0.3 kg m^2
PV system maximum power	P_{PV}	600 w
PV system efficiency	η_{PV}	90%
Motor efficiency	η_m	90%
SAPHT overall efficiency	η_{SAPHT}	62%

$$F_{res} = C_{roll} . M_{tot} . g . \cos\alpha + \frac{1}{2} \rho A C_d (V + V_w)^2 + M_{tot} . a_{lacc} + I . \frac{G^2}{r^2} . a_{lacc} + M_{tot} . g . \sin\alpha + F_{drawbar} \quad (3)$$

Where F_{roll}, F_{air}, F_{acc}, F_{hill}, and $F_{drawbar}$ denote the rolling resistance, aerodynamic drag, acceleration, hill climbing, and drawbar forces, respectively. C_{roll} is wheel rolling resistance coefficient; g is gravity acceleration; ρ, C_d, A, and V_w are air density, drag coefficient, frontal area, and wind velocity, respectively. M_{tot} is vehicle total mass; a_{lacc} is wheel linear acceleration; I is the moment of inertia of the wheel and electric motor; G is gear ratio from the electric motor to the wheel drive shaft; r is the drive tire radius; α is the road or field slope. Considering the speed (V) and the required traction force (F_{tr}), the vehicle requested power (P_m) from the electric motor side could be then expressed as:

$$P_m = F_{tr} V / \eta_m \eta_t \quad (4)$$

Where η_m and η_t denote the motor and transmission average efficiency, respectively. Therefore, the battery pack power ($P_{Batt.}$) can be calculated as follows:

$$P_{Batt.} = P_m + P_a + \frac{P_{PTO}}{\eta_{PTO}} - P_{Genset} - \eta_{PV} . P_{PV} \quad (5)$$

Where P_a, P_{PTO}, $P_{Bio\text{-}Gen}$, and P_{PV} are the accessory power, PTO system propulsion power, Bio-Gen power, and PV array power, respectively. In addition, η_{PV} and η_{PTO} denote the PV system and the PTO system efficiency.

2.4. Energy Storage System (Battery)

To handle desired loads, it is essential that the total power of the Bio-Gen, the PV array, and the battery pack are greater than the maximum rated power of the electric motors at any accepted time within the range of operation. As well as that, it is necessary to assure that the battery energy quantity lies between its maximum and minimum limits [21]. SOC is one of the most important parameters of the battery. Because not only does it inform a driver about the amount of remaining charge and mileage, but also it is a parameter that needs to be carefully monitored to avoid damage that can be caused by overcharging/discharging the battery. However, many research has been done to estimate the amount of battery SOC ($SOC_{Batt.}$) that is beyond the scope of this research [22]. Hence, coulomb counting based on current integration remains one of the most commonly used methods due to its reasonable accuracy and implementation simplicity that is represented by the following equation [23]:

$$SOC_{Batt} = SOC_{Init.} - \frac{100}{3600\, Q_{Batt.}} \int_0^t I_{Batt.}\, dt \quad (6)$$

Where $SOC_{Init.}$ is initial SOC of the battery, $Q_{Batt.}$ and $I_{Batt.}$ are battery capacity and current, respectively. Since the purpose of this paper is not the battery surveying, the lead-acid battery model presented by [24] is considered using the parameters found in [25]. In addition, relationship in [26] used to determine total battery power ($P_{Batt.}$) from the battery characteristics manufactory SOC lookup table as:

$$P_{Batt.} = V_{OC} . I_{Bat.} - I_{Bat.}^2 . R_{Batt.} \quad (7)$$

Where $R_{Batt.}$ and V_{OC} are resistance from experimental tests and open-circuit voltage of the battery. The Kirchhoff's current law is used to model the parallel connection between the battery pack, traction subsystem, PTO system, Bio-Gen, and PV system:

$$I_{Batt.} = I_{TS} + I_{PTO} - I_{PV} - I_{Bio\text{-}Gen.} \quad (8)$$

Where I_{TS} and I_{PTO} donate the requested currents respectively from the traction system and the PTO system current, I_{PV} and $I_{Bio\text{-}Gen}$ are supplied currents by the PV system and the Bio-Gen unit. Output power and input power from the battery considered with negative and positive signs, respectively. Therefore, the power delivered by the Bio-Gen and PV array is regarded as positive. The total energy of the battery ($E_{Batt.}$) can be evaluated in terms of a time integral function of $P_{Batt.}$:

$$E_{Batt.} = \eta_{Bat.} \left(\int_0^{t1} \eta_{PV} . P_{PV}\, dt + \int_0^{t2} \eta_{\text{Bio-Gen}} . P_{\text{Bio-Gen}}\, dt - \int_0^{t3} 2P_m\, dt - \int_0^{t4} \frac{P_{PTO}}{\eta_{PTO}}\, dt \right) \quad (9)$$

Where $\eta_{Bat.}$ and $\eta_{Bio\text{-}Gen}$ donate the battery pack and Bio-Gen efficiency; t_1, t_2, t_3, and t_4 are charging-discharging time intervals for the PV array, the Bio-Gen, the propulsion motors, and PTO motor, respectively.

Indeed, the battery is charged mainly when the vehicle is plugged into on-Farm electricity supply (renewable source). The battery initial $SOC_{Init.}$ is estimated according to the open-circuit voltage and the battery left for 24h before the measurement. It is assumed that the battery is fully charged at the beginning of the work, and the suggestion is that the battery SOC should be at the minimum level (SOC = 20%) at the end of the working day.

2.5. Power Electronics, Mechatronic and PV System

The electric machines and power electronics components, such as converters and motors drive, are modelled based on the experimental lookup table data provided by the manufacturers; that determines the electric motors torque, speed, and related efficiency [27]. For example, the on-board PV system with approximately 6m^2 polycrystalline panels and 660 W peak power (W_p) were provided [21]. Based on the data from National Renewable Energy Laboratory (NREL) website (2019, [28]), the average amount of hourly available PV power in Karaj, Iran (latitude 35° 48′ N, longitude 50° 58′ E ,where the project was performed), applied as the PV system model. In Iran, agricultural operations are usually performed from April to September. The experimental field tests were conducted in June 2018 with zero-degree slope of the PV panel. Therefore, the average hourly solar power on June 15th 2018, applied to the model as a lookup table i.e., seen in Fig.2.

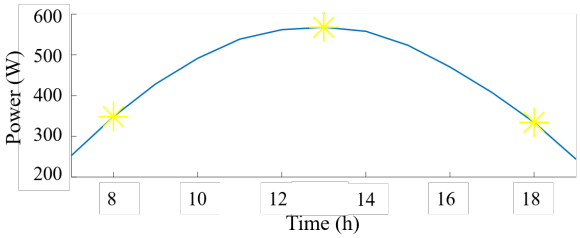

Fig. 2. Calculated average hourly solar energy on 15th June applied to model [28].

2.6. Bio-Gen System

An analytical Bio-Gen model is difficult to obtain. It is, therefore, common to use the map to describe the ICE fuel consumption. One important map is the brake specific fuel consumption (BSFC) map. This map can be determined by empirical procedures on an engine test or can be computed by some software packages [29]. The fuel consumption of the engine ($\dot{m}_{gas}$) is given by a steady-state map as a function of engine torque (T_{ICE}) and engine speed (ω_{ICE});

$$\dot{m}_{gas} = f\,(T_{ICE}, \omega_{ICE}) \qquad (10)$$

The power consumed of the Bio-Gen ($P_{Bio\text{-}Gen}$) can be computed from the fuel Lower Heating Value (LHV_{gas}) as follows expressions;

$$P_{Genset} = LHV_{gas} \cdot \dot{m}_{gas} \cdot \eta_{Genset} \qquad (11)$$

The *BSFC* can be used for comparing the efficiency as follows;

$$BSFC = \frac{\dot{m}_{gas}}{P_{\text{Bio-Gen}}} \qquad (12)$$

In order to take into account the added on-board energy source, the State-of-Charge of the biogas tank (SOC_{gas}) is estimated from the initial mass of biogas ($V_{gas-init}$) by following relationship;

$$SOC_{gas} = \frac{m_{\text{gas-init}} - \int_0^t \dot{m}_{gas}\, dt}{m_{\text{gas-init}}} \qquad (13)$$

The ICE nominal power depends on the vehicle specifications and vehicle application. Likewise, the average daily energy requirement allows to sizing of the battery as well as the RE. However, the Bio-Gen of an E-REV design to provide average power during the extended driving range [1]. In this case, the required energy ($E_{req.}$) for the vehicle and the attached machine would be drawn from the battery, the PV system, and the Bio-Gen.

$$(E_{Batt.} + E_{\text{Bio-Gen}} + E_{PV})\,\eta_{SAPHT} \geq E_{req.} \qquad (14)$$

Where $E_{Batt.}$ is the maximum rated energy of the battery, $E_{Bio\text{-}Gen}$ is the nominal produced energy of the Bio-Gen, E_{PV} is the average energy generation of the PV system, and η_{SAPHT} is the total average efficiency of the SAPHT powertrain (62%). Using the developed energy model, we can calculate how much energy is needed to work in a given working condition. Consequently, by using simulation can estimate how much energy is needed for a specific period (e.g., during a working day). Finally, considering the available energy of the on-board battery and the PV system, the range-extender capacity (required power and fuel tank capacity) can be sized.

In order to the RE sizing simplicity, a set of constraints should be considered in the model. All-Electric Range (AER), grade ability, and acceleration time have been considered as the most important constraints in the literature [1]. It is assumed that the E-RSAPHT reaches its operational velocity with constant acceleration and the power rate during the operation. Then, the acceleration and corresponding torque become zero. The drive system of the SAPHT is designed to prevent sudden acceleration by the use of a high pedal disable (HPD) function, which controls the SAPHT to start from a stop and reach the final velocity in 10s approximately [21]. Therefore, the constant acceleration of 0.75 m/s^2 is obtained.

On the other hand, multiple power sources of series PHEVs architecture allow the Bio-Gen to operate in its high-efficiency region (recommended by the manufactory instruction) with a near-optimal fuel consumption rate. Therefore, it could be considered that the electrical output power of the Bio-Gen is constant. Furthermore, as mentioned earlier, charging a battery from the grid during the night is more efficient than charging it via on-board Bio-Gen; consequently, it seems to be acceptable to hybridize the tractor with downsized Bio-Gen. Hence, with respect to the design objective for agricultural light applications, a Bio-Gen with 389 cc displacement was developed and converted to use biogas due to its power-to-weight ratio and size. According to manufactory data, the maximum power that the engine can handle is around 13Hp at the nominal speed of around 3600 RPM and this lightweight engine is designed originally for fuelling by the natural gas and biogas. In addition, the generator was coupled on the same shaft without the reduction gear and its rated power of 4.4kW. The technical specifications of the engine and the main components of the gas system are given in Table 2. The upgraded biogas selected as a renewable fuel allows fuel flexibility as well as potentially zero emissions when compared to the fusil fuels. An on-board battery charger was used to convert the 220VAC electricity from the grid and Bio-Gen output power to an appropriate DC voltage to charge the battery pack. By considering 0.9 efficiency in the converter, the average amount of the supplied current and voltage measured under 50A and over 80 V, respectively.

Table 2. Some specifications of installed Bio-Gen.

Engine-generator Model	NGCC5000
Rated Power(kW)	4.4
Rated Rotating Speed(r/min)	3600
Displacement (CC)	389
Engine rated power (HP)	13
Starting Mode	Electric Starter
Fuel Consumption (Rated Power)	NG: 0.35 m3/kWh
Weight (kg)	93
Biogas storage capacity (kg)	14

2.7. Energy Management Strategy

The PHEV's power distribution flexibility carries with a more complicated EMS. Many studies have been concentrated on it in the literature [30]. The control strategies are broadly classified into optimization-based and rule-based strategies. Optimal control strategies like as model predictive control, genetic algorithm and dynamic programming are frequently used offline to explore the fuel economy potential in the literature, though yet have not been massively used for practical application. On the other hand, rule-based methods, due to easier implementation and reliability, are widely used in real-time vehicular control systems. Generally, four working modes are supposed for the PHEVs namely electric vehicle (EV), charge-sustaining (CS), charge depletion (CD) modes, and charge-blending (CB). The fuel consumption comparison is resulted from these rule-based and optimization control strategies in [31] showed that the charge-blending control mode with proper control parameters produces the lowest fuel consumption among the rule-based ones.

Usually, PHEVs have a predefined SOC operating range (e.g., 90% to 20%) to maximize battery life [1]. On the other hand, since the biogas must be pressured in relatively bulky and massive tanks, and the farm might be far from the refuelling station; design constraints need to be taken into EMS considerations with the intention to minimize battery degradation and fuel consumption. Consequently, an innovative supervisory control algorithm is developed and implemented to the E-RSAPHT. The following design considerations are established for these strategies:

a) According to [32] the minimum degradation can be achieved if the SOC is maintained between 40% to 75%. Therefore, the batteries SOC is considering limited to 20 - 100%.

b) Considering when the Bio-Gen is ON and the output power is constant.

c) Considering when the SOC_{gas} is 10% and the fuel tank is empty.

The proposed strategy is designed with an attempt to maintain the battery SOC near the lower value at the end of the working day while being charging by stationary renewable energy sources during the night. The flowchart of the proposed controller is presented in Fig.3.

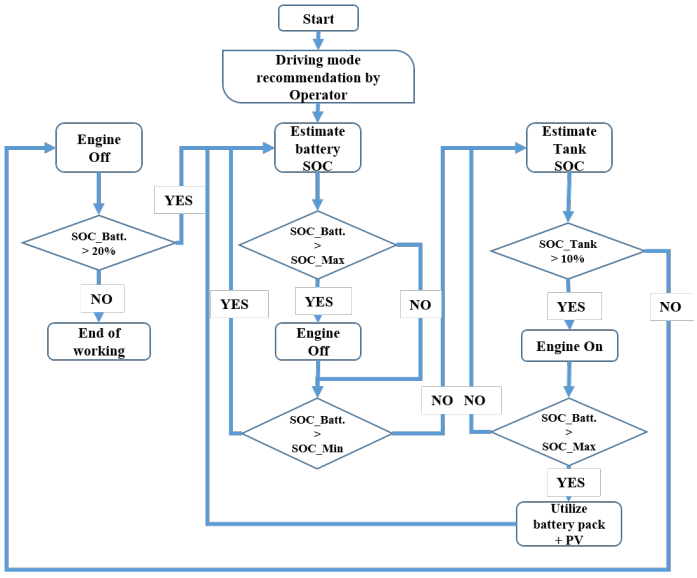

Fig. 3. Supervisory Control Strategy for the E-RSAPHT.

At first, three working modes (Economic, Normal and High-power) are suggested by the EMS. Table 3 demonstrates the considered battery SOC thresholds and average energy requirement for different working modes; these thresholds are defined based on energy requirements by the aim of the energy model. After that, tractor operator can determine the working mode according to the average required energy ($E_{Ave.}$) and the working time from the measured data for each farm operation classified from the author's previous research [21]. In this case, for new types of machines, the tractor operator just needs to choose the working mode according to the average required power range from the equipment manufacturer for better efficiency. To obtain diverse operational modes, the supervisory controller checks the battery SOC when the vehicle is started:

• If the battery SOC is equal or greater than *SOC_Min*, the battery and PV system are used to propel the vehicle;

• If the battery SOC is below *SOC_Min*, check the SOC of biogas tank (SOC_{gas}). If SOC_{gas} is larger than 10%, the Bio-Gen will be activated to give out constant output power to charge the battery or provide power to propel the tractor; when the battery SOC reaches *SOC_Max*, the Bio-Gen turns off;

• Fuel tank charging is terminated if the (SOC_{gas}) is lower than 10%; and, the E-RSAPHT will stop if the SOC of the battery is subordinate than 20%.

Table 3. The Battery SOC thresholds for different working modes.

Working mode	Average energy requirement (Wh)	*SOC_Min*	*SOC_Max*
Economic	$E_{Ave.} < 5000$	55%	75%
Normal	$5000 =< E_{Ave.} < 8000$	65%	85%
High-power	$E_{Ave.} >= 8000$	75%	95%

3. Experimental Setup

3.1. Design EMS Electronic Module

The main goal of this project is the design and development of a renewable-based E-RSAPHT with a reasonable range and efficiency. Therefore, the developed algorithm was applied in designed EMS electronic module to control the operation of the RE on the safe operating condition. Figure 4 is shown a simplified architecture block diagram of the manufactured EMS board.

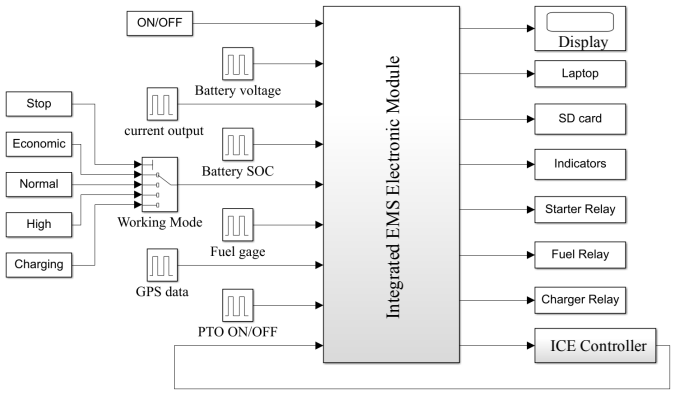

Fig. 4. A simplified architecture block diagram of the integrated EMS electronic module.

The inputs of the controller board are from the units like current sensors, voltage-measuring modules, working mode switch, etc. These inputs are processing in the EMS and the output commands are commanding to the engine controllers to drive the Bio-Gen. The measured current is processed by the EMS to estimate the SOC of the batteries. From the operator module, it is just necessary to determine the working mode of the operation (Economic, Normal or High) for more efficient performance. The vehicle status such as the operation mode, SOC, and voltage of the battery pack are visible in the display unit. In addition, the E-RSAPHT velocity and global position are measured by using a GPS module. A module was designed for collecting the driver commands and measuring the parameters into a portable computer and SD card.

An additional module was developed to control the Bio-Gen starter and fuel flow and charging system. Depending on the determined working mode by the operator, the EMS would provide enough power to propel the vehicle. For the control strategy, the battery pack is the major energy source to power the electric vehicle, while the RE gives out certain power output to propel the E-RSAPHT and charge the battery. The RE will be turned ON when the SOC of the battery is less than the given minimum threshold and shuts down when the SOC is above a predefined threshold. When the Bio-Gen is turned ON, an on-board single-phase charger inverts the power into an appropriate DC voltage to charge the battery pack. However, the vehicle runs with a battery pack and PV system when the Bio-Gen is OFF.

3.2. Experimental Cycle Measurement and Derivation

After programming the EMS with the control algorithm and initial round of testing, the E-RSAPHT performance was tuned under different load conditions. The project carried out at Mechanical Engineering of Biosystems's department, the University of Tehran as a case study (Karaj, Iran). Fig. 5 shows the E-RSAPHT in the experimental tests.

According to reviewed papers, there is no specific available standard working cycle for evaluation of electric farm tractors until now. However, an agricultural tractor usually works during the day with repetitive operations; hence, it could be categorized in transportation and field works. In transportation application, the tractor is usually used to haul the trailer on rural roads or field. On the other hand, in fieldwork such as spraying, traction and PTO systems might be used simultaneously to drive the machine. In addition, in stationary operations cases like as pumping and threshing, only the rotating force of the PTO system might be used. Therefore, in this research, the authors defined several real-world particular working cycles to assess the E-RSAPHT performance under different loads with diverse average velocity and required power. To simplify the process, three typical predefined common working modes are designed at constant parameters in flat grand as seen in Table 4.

(a) (b)

Fig. 5. The E-RSAPHT in real-world field experiments with typical implements: (a) Prototype tractor cruising, and (b) Trailer pulling.

Table 4. Predefined farm operation characteristics for experimental tests.

Farm duty	Typical implement	Speed range (km/h)	Machine weight (kg)	PTO speed (rpm)	Average C_{roll}
Driving at road	Trailer	0 - 25	2000	0	Asphalt (0.029)
Driving at repetitive continuously move and stops in the field	Boom-type sprayer	0 - 10	400	540	No-tilled field (0.052)
Stationary operations with PTO	Water-pump	0	0	540	0

The field experiments were conducted with three particular implements: trailer (traction load), boom-type sprayer (traction and PTO load) and water-pump (PTO load) in June 2018 at a special testing farm. In fact, these real-world working cycles contain different contributions of light, medium, and high-power demand working conditions based on measured data form author's previous research work [21]. Figure 6 shows typical predefined route and speed profile by the boom-type sprayer in a particular testing field. Finally, the measured data from the real-time experiments were used to analyse the developed system under different farm operations condition.

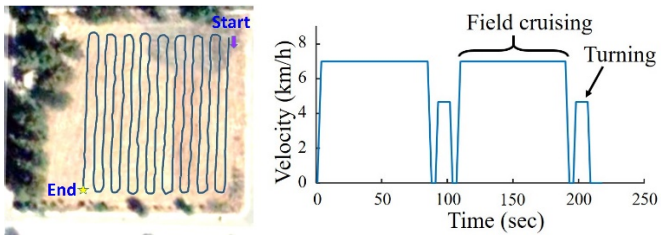

(a) (b)

Fig. 6. (a) predefined testing route for sprayer working cycle, and (b) speed profile.

4. Results and Discussions

4.1. Model Validation and Simulation Results

To validate the established model and developed algorithm, at the first step the simulation has been carried out based on NEDC by considering a fully charged battery (initial SOC supposed 100%). Here the NEDC is used as the target condition in the simulation with the trailer working condition, which aims to simulate stop-and-go rural driving conditions. To comply with the 25 km/h speed limitation of the vehicle, the NEDC had to be scaled down, so that the top speed demanded by the cycle did not exceed due to the SAPHT's limits. Figure 7a proves that the forward simulation model follows the scaled reference driving cycle in high precision. Therefore, the model can be used as the basis for the vehicle EMS evaluation and range analysis simulation before implementation. In addition, the average traction power of the cycle calculated 7.92 kW from the simulation results (Fig.7b).

Since this work revolves around battery discharge and their ensuing degradation for PHEV, the NEDC was simply to loop the cycle end-to-end to reach 20% of battery SOC. Because of the battery's discharge behaviour, the total range of the vehicle could be extrapolated overtime under these working conditions. The results of EV mode and charge blending (CB) mode simulation by scaled-down NEDC is shown in Fig.8. It is obvious that with full charge existing battery pack the AER of the basic system in the EV mode (without allowing to turn on the Bio-Gen) obtained up to 6000s (+1.67h) to reach the final 20% SOC of the battery pack. However, when using the rule-based EMS in a CB mode (allowing to turn on the downsized Bio-Gen), the operating range increased to over 10000s (+2.8h). These simulation results also indicate that a Bio-Gen with about 10 kW rated power is able to supply the existing system power for about 10 hours of continuous operation in scaled-down NEDC. Furthermore, these results show that the proposed algorithm was aimed at increasing the working hours range, as well as prolonging the battery lifetime to acceptable levels. As a result, due to the possibility of using a downsized engine in optimal RPM in the series HEVs, less fuel would be used compared to conventional tractors in this category.

Moreover, simulation results in Fig.9a shows the motor required power for moving a trailer at constant speed of 25 km/h with a two-ton load on an asphalt road with 10 km/h opposing wind velocity. It is obvious that in the bingeing, required power for acceleration (+45kW) was more than four times compared to the constant speed. As a result, as it can be seen in the graph, a +11.32 kW average traction power is required. This calculated quantity is close to the experimental result with the basic system. In addition, Fig.9b shows the full charge battery SOC deviation against the required energy during the simulation. It can be found that with a full charge of the existing battery pack, the AER in 4000s (under 27 km) would reach the final 20% SOC of the battery pack.

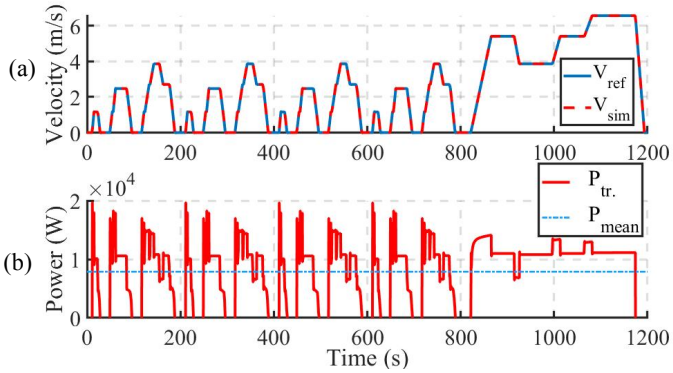

Fig. 7. Simulation results for; a) the reference scaled-down NEDC compared to Simulink results b) electric motor power demanded.

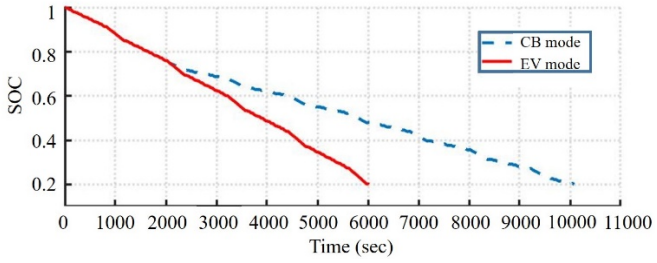

Fig. 8. Simulation results of CD mode and CS mode in scaled-down NEDC to battery depletion with the trailer pulling operation mode.

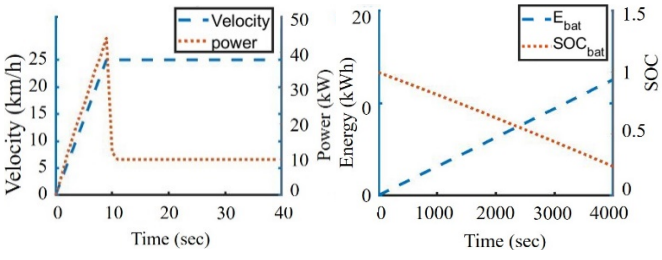

(a) (b)

Fig. 9. Simulation modelling results in EV mode when the vehicle is cruising to 25 km/h.

4.2. Experimental Working Cycle Analysis

In this section, the results of experimental tests for the developed E-RSAPHT with different typical farm operations are presented. Figure 10 shows real world measured velocity, battery current, battery voltage, and demanded power in trailer pulling operation. These data illustrated that the velocity range was under 25 km/h depending upon the road conditions and farm operation situation. This figure also presents the required power from multiplying the measured current and voltage that is related to vehicle speed and required torque during the operation. Also, the average required power obtained 8.63 kW from the trailer working cycles after several repeats, which matches the reported data in [21]. Consequently, the high-power mode would be selected for EMS in trailer working conditions.

Fig.10b shows that the start-up currents of the electric motors were up to 400 Amps, which is subsided several times of the normal current for a few seconds. The reason could be found in the vehicle required power for acceleration and the characteristics of electric motors. This is obvious that the battery voltage fluctuations occurred depending on the consumption current while the voltage level decreased by the energy consumption during the test. From the graphs, we can see that again the battery suddenly supplied higher currents when the battery voltage was decreased immediately. Furthermore, this shows the battery voltage increased during the stop mode due to enough time for battery energy recovery.

Figure 11 shows the other experimental measured working cycle in boom-type sprayer operation conditions based on predefined working cycle in Fig.6a. From Fig.11a, it is obvious that the velocity range in this cycle obtained up to 7.2 km/h depending on the farm conditions. Figure 11b illustrates the mixed required power from the traction force, and electrical PTO power in boom-type sprayer operation. The results from several repeat field tests with the boom-type sprayer acquired 5.37 kW and 1.59 kW power by traction system and PTO system respectively, which lead to 6.96 kW total average required power in this cycle. Consequently, the normal mode (see Table 3) seems to be an appropriate mode for this working cycle.

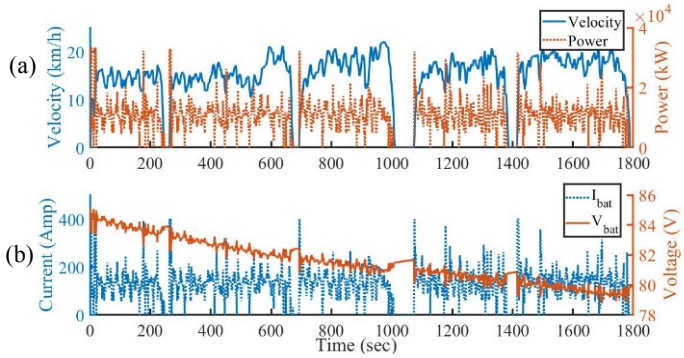

Fig. 10. Measured experimental data during the Trailer working operation by the E-RSAPHT (a) Velocity and required power, (b) battery output current and voltage.

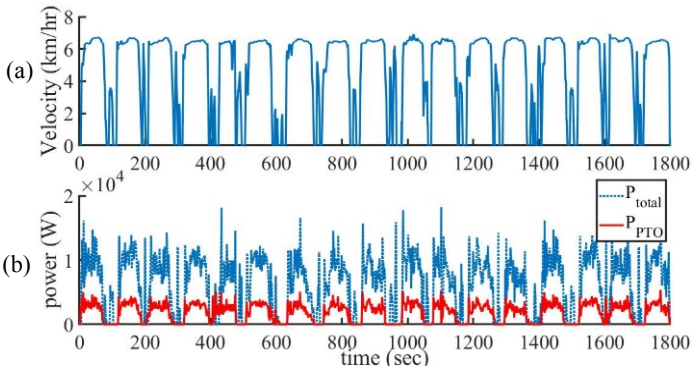

Fig. 11. Measured experimental data during the boom-type sprayer working cycle by the E-RSAPHT, (a) velocity, (b) overall required power and PTO system required power.

By comparing the working cycle between the Fig.10 and the Fig.11, it will appear that in the trailer cycle, the travel distance is usually longer than boom-type sprayer one and there were long stops, due to road and farm work conditions. While in the boom-type sprayer, it turns out that the operations are almost repetitive and the work cycles are almost similar. However, it should be taken into account that the PTO does not work at the end turn, and the speed of work is much reduced. In addition, in operations, like water-pump, that are done at a stationary mode by the PTO system; an electrified powertrain is able to decrease the idle power losses and minimize fuel consumption.

4.3. Range Analysis

An E-RHEV's working range is linked to various variables such as ESS capacity, RE running time, energy consumption under different working cycles and driving behaviours. Figure 12 compares the E-RSAPHT performance under high-power mode (see Table 3) with an 80% initial battery SOC level. Figure 12a illustrates the comparative range between the CD mode and CS mode. The dashed line shows the SOC changes when RE is activated while the dotty line displays the battery SOC deviation in pure electric mode. This result represents at least 10% SOC level difference between the two modes during the 1800s driving in the trailer working cycle. From Fig.12b, this is obvious that when the battery SOC level is going under 75%, Bio-Gen will be triggered to help the battery pack in power supplying. Indeed, the EMS increased 10 percent of the battery SOC during 1500 seconds for 750 grams of renewable fuel by activating the Bio-Gen.

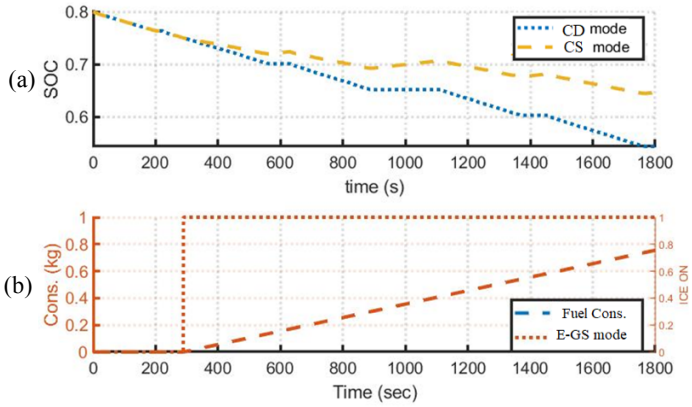

Fig. 12. Experimental results in high-power mode during the trailer working condition by developed EMS (a) Battery SOC, (b) Bio-Gen mode, and fuel consumption.

Table 5 compares the performance results of the three typical farm operations by the developed E-RSAPHT. Average velocity obtained 12.36 km/h and 6.24 km/h in the Trailer and Boom-type sprayer working cycles during the test, respectively. This is obvious that the trailer working cycle requires much more power due to more weight and velocity compared to the other ones. Furthermore, the result illustrates that 4.31, 3.04, and 2.1 kWh electrical energy have been consumed during the 1800s testing with trailer, Boom-type Sprayer and Water-pump working cycles, respectively. These results are also consistent with the reported field experiment tests by the primary system [21]. From these results, it becomes clear that about one quarter (26%) of the total battery energy has been consumed during the 1800s test by the Trailer working cycle. The final SOC amount for the boom-type sprayer was lower due to later start ON of the ICE in moderate mode and the simultaneous use of the PTO. This is obvious that by utilizing the developed RE and the proposed EMS, the battery SOC depleting rate has decreased. However, in the Water-pump mode due to the EMS strategies and low energy consumption, the Bio-Gen was not turned ON during this same test time. The biogas consumption during the Trailer and Boom-type sprayer test was 750 and 160 grams, respectively.

Table 5. The experimental test performance results for the predefined farm operation.

Farm operation type	Unit	Trailer	Boom-type Sprayer	Water-pump
Test time	s	1800	1800	1800
Average velocity	km/h	12.36	6.24	0
Distance travelled	km	6.18	2.86	0
Average power requirement	kW	8.63	6.96	4.2
Total energy consumption	kWh	4.30	3.04	2.1
Initial battery SOC	%	80	80	80
Final battery SOC in CD mode	%	54	61	67
Final battery SOC in CS mode	%	65	64	67
Delta SOC between CD and CS modes	%	11	3	0
Fuel consumption	kg	0.75	0.16	0

However, experimental tests have many limitations and the 1800 seconds tests were found to be too brief to provide an appropriate measure of total range. The solution proposed was simply to loop these cycles to reach 20% of battery SOC in different powertrain by importing the measured data to the developed Simulink model. Considering the energy generated by the Bio-Gen, collected by the PV array and provided by the battery pack, the total available energy calculated up to 63.45 kWh per day. Using this energy, the E-RSAPHT could operate the Trailer, Boom-type sprayer, and water-pump for 7.3, 8.7, and 14h at the specified conditions, respectively. In addition, results in Table 6 showed that by using the Bio-Gen, operating time ranges were increased by 4.8, 5.3, and 9.7h, respectively for the Trailer, Boom-type sprayer, and Water-pump operation compared to the basic pure electric system. Moreover, the result in Table 6 shows that the Bio-Gen will produce 32.12, 37.38, and 37.65 kWh during these cycles that include almost 65.7%, 60.9%, and 68.8% of the total energy consumed. However, the fuel consumption in the trailer, Boom-type Sprayer and Water-pump operation modes calculated 12.85, 14.9, and 15 kg, respectively. Finally, from these results, it could be calculated that the on-board PV array provides almost 6.87%, 6.61%, and 8.96% of the total energy consumed during the Trailer, Boom-type Sprayer and Water-pump operation modes, respectively.

Table 6. Comparative working range in the different farm operation conditions.

Farm operation type		Trailer	Boom-type Sprayer	Water-pump
CD mode time range (basic system)	hr.	2.5	3.4	4.4
CS mode time range	hr.	7.3	8.7	14.1
Final battery SOC in CS mode	%	20	20	27
Total Bio-Gen produced energy	kWh	32.12	37.38	37.65
Produced energy from biogas	%	65.7	60.9	68.8
Total fuel consumption	kg	12.8	14.9	15
Total PV produced energy	kWh	3.36	4.15	5.73
Produced energy from PV	%	6.87	6.61	8.96

5. Conclusion

This paper introduces the process of modelling, simulation, and implementation of E-RSAPHT, which is meant to be used in agricultural light applications as an independent energy Off-Road vehicle. In this regard, a realistic MATLAB-Simulink model was developed to perform feasibility studies to design the EMS and Bio-Gen. Moreover, some experiment working cycles were defined and conducted in the field to derive typical farm working cycles. Simulation results based on the measured data from the

experimental tests, found that an 8.63 kW net traction power is required to cruise the vehicle with a two-tone trailer load at 25 km/h constant speed. However, because of series drivetrain architecture of this case study work, an appropriate downsize 4.4 kWh biogas-fuelled RE was developed to charge sustaining battery pack by the aid of the PV system.

In addition, an EMS circuity was developed to implement the supervisory control strategy according to the required power and SOC. Considering the economic, normal, and high-power modes by the proposed strategy, the EMS has determined the thresholds to keep the SOC between 20% and 80%. The control strategy evaluated on the powertrain model through the field experiment. The results showed that the designed strategy is significantly more effective for the E-RSAPHT performance on the prescheduled working cycles.

In this research, the developed vehicle was validated in three typical implements through defined working cycles during the day. The actual field tests results showed that the operating time ranges of the E-RSAPHT increased up to 7.3, 8.7, and 14h that equals to 292, 255, and 320% by the Trailer, Boom-type sprayer, and water-pump, respectively, compared to the basic pure electric system.

These results prove that the developed farm vehicle had satisfactory performance under the tested equipment. Furthermore, the E-RSAPHT with 4.4 kW Bio-Gen and 0.6 kW PV system supplied the required power compared to a conventional system using several tens of kilowatts gasoline ICE. Moreover, in case of access to on-site biogas refuelling infrastructure, the E-RSAPHT energy storage systems are able to be recharged without any need of fossil fuel.

Although this work has well improved the characteristics of the developed E-RSAPHT as an independent farm vehicle, some prospects for extending the scope of this work remains as follows:

- Incorporating farm operation condition recognition algorithm into the presented system to reach an intelligent holistic automated control strategy.
- Considering economic aspects and life-cycle assessment of the developed system compared to conventional farm vehicles.
- Exergetic efficiency analysis of the developed vehicle powertrain.
- Improving some driving mechanism in order to reach more efficient powertrain, e.g., designing a hydraulic system with an accumulator mechanism for the ease of operation with a three-point connecting lift system.
- Concatenating the force regenerative system to recover the wasted force from the traction and PTO systems.
- Performing a lifetime and supplied power changing of the energy sources under the developed system.

References

[1] M. Ehsani, Y. Gao, S. Longo, and K. Ebrahimi, *Modern electric, hybrid electric, and fuel cell vehicles*. CRC press, 2018.

[2] Z. Cerovsky and P. Mindl, "Impact of Energy Production Technology on gas emission by Electric Hybrid and Electric Vehicles," *International Journal of Renewable Energy Research,* vol. 1, no. 3, pp. 118-125, 2011.

[3] (2016). *European Stage V Non-Road Emission Standards*.

[4] G. Moreda, M. Muñoz-García, and P. Barreiro, "High voltage electrification of tractor and agricultural machinery–a review," *J Energy Conversion Management,* vol. 115, pp. 117-131, 2016.

[5] A. Ghobadpour, L. Boulon, H. Mousazadeh, A. S. Malvajerdi, and S. Rafiee, "State of the art of autonomous agricultural off-road vehicles driven by renewable energy systems," *Energy Procedia,* vol. 162, pp. 4-13, 2019.

[6] H. Mousazadeh, "A technical review on navigation systems of agricultural autonomous off-road vehicles," *Journal of Terramechanics,* vol. 50, no. 3, pp. 211-232, 2013.

[7] C. Mi and M. A. Masrur, *Hybrid electric vehicles: principles and applications with practical perspectives*. John Wiley & Sons, 2017.

[8] P. Tritschler, S. Bacha, E. Rullière, and G. Husson, "Energy management strategies for an embedded fuel cell system on agricultural vehicles," in *Electrical Machines (ICEM), 2010 XIX International Conference on*, 2010, pp. 1-6: IEEE.

[9] B. Xie, H. Li, Z. Song, and E. Mao, "Powertrain system design of medium-sized hybrid electric tractor," *J Inf. Technol. J,* vol. 12, no. 23, pp. 7228-7233, 2013.

[10] M. Gonzalez-de-Soto, L. Emmi, C. Benavides, I. Garcia, and P. Gonzalez-de-Santos, "Reducing air pollution with hybrid-powered robotic tractors for precision agriculture," *Biosystems Engineering,* vol. 143, pp. 79-94, 2016.

[11] I. Cetinbas, B. Tamyürek, and M. Demirtas, "Energy Management of a PV Energy System and a Plugged-in Electric Vehicle Based Micro-Grid Designed for Residential Applications," in *2019 8th International Conference on Renewable Energy Research and Applications (ICRERA)*, 2019, pp. 991-996: IEEE.

[12] M. Kabir *et al.*, "Research trends for performance, safety, and comfort evaluation of agricultural tractors: A review," *Journal of Biosystems engineering,* vol. 39, no. 1, pp. 21-33, 2014.

[13] W. Yaïci, L. Kouchachvili, E. Entchev, and M. Longo, "Dynamic Simulation of Battery/Supercapacitor Hybrid Energy Storage System for the Electric Vehicles," in *2019 8th International Conference on Renewable Energy Research and Applications (ICRERA)*, 2019, pp. 460-465: IEEE.

[14] D. Karner and J. Francfort, "Hybrid and plug-in hybrid electric vehicle performance testing by the US Department of

Energy Advanced Vehicle Testing Activity," *Journal of Power Sources,* vol. 174, no. 1, pp. 69-75, 2007.

[15] R. M. Hoy, R. Rohrer, A. Liska, J. D. Luck, L. Isom, and D. R. Keshwani, "Agricultural industry advanced vehicle technology: Benchmark study for reduction in petroleum use," Department of Energy National Laboratory U.S.2014.

[16] F. Martel, Y. Dubé, L. Boulon, and K. Agbossou, "Hybrid electric vehicle power management strategy including battery lifecycle and degradation model," in *2011 IEEE Vehicle Power and Propulsion Conference*, 2011, pp. 1-8: IEEE.

[17] S. S. Raghuwanshi and R. Arya, "Economic and Reliability Evaluation of Hybrid Photovoltaic Energy Systems for Rural Electrification," *International Journal of Renewable Energy Research,* vol. 9, no. 1, pp. 515-524, 2019.

[18] R. O. Magalhães *et al.*, "Review on applications of electric vehicles in the countryside," *Ciência Rural,* vol. 47, no. 7, 2017.

[19] A. Evans, V. Strezov, and T. J. Evans, "Sustainability considerations for electricity generation from biomass," *Renewable sustainable energy reviews,* vol. 14, no. 5, pp. 1419-1427, 2010.

[20] IRENA, "Biogas for road vehicles: Technology brief," ed: International Renewable Energy Agency Abu Dhabi, 2017.

[21] H. Mousazadeh, A. Keyhani, A. Javadi, H. Mobli, K. Abrinia, and A. Sharifi, "Optimal power and energy modeling and range evaluation of a solar assist plug-in hybrid electric tractor (SAPHT)," *J Transactions of the ASABE,* vol. 53, no. 4, pp. 1025-1035, 2010.

[22] Y. Sone *et al.*, "Charge and discharge performance of over-discharged lithium-ion secondary battery—Lessons learned from the operation of the interplanetary spacecraft HAYABUSA," *J Electrochemistry,* vol. 75, no. 12, pp. 950-957, 2007.

[23] K. S. Ng, C.-S. Moo, Y.-P. Chen, and Y.-C. Hsieh, "Enhanced coulomb counting method for estimating state-of-charge and state-of-health of lithium-ion batteries," *J Applied energy,* vol. 86, no. 9, pp. 1506-1511, 2009.

[24] M. Ceraolo, "New dynamical models of lead-acid batteries," *IEEE transactions on Power Systems,* vol. 15, no. 4, pp. 1184-1190, 2000.

[25] H. Mousazadeh, A. Keyhani, A. Javadi, H. Mobli, K. Abrinia, and A. Sharifi, "Evaluation of alternative battery technologies for a solar assist plug-in hybrid electric tractor," *Transportation Research Part D: Transport Environment,* vol. 15, no. 8, pp. 507-512, 2010.

[26] S. Dhameja, *Electric vehicle battery systems*. Elsevier, 2001.

[27] A. Belkaid, I. Colak, K. Kayisli, and R. Bayindir, "Design of an Intelligent Peak Power Converter for Solar Plants with Lead–acid Battery," in *2018 7th International Conference on Renewable Energy Research and Applications (ICRERA)*, 2018, pp. 1400-1406: IEEE.

[28] N. R. E. L. (NREL). (2019). *Estimation of the energy production for of grid-connected photovoltaic (PV) energy systems*. Available: https://www.nrel.gov/

[29] T. J. Böhme and B. Frank, *Hybrid Systems, Optimal Control and Hybrid Vehicles*. Springer International, 2017.

[30] S. G. Wirasingha and A. Emadi, "Classification and review of control strategies for plug-in hybrid electric vehicles," *IEEE Transactions on vehicular technology,* vol. 60, no. 1, pp. 111-122, 2011.

[31] X. Wang, H. He, F. Sun, X. Sun, and H. Tang, "Comparative Study on Different Energy Management Strategies for Plug-In Hybrid Electric Vehicles," *Energies* vol. 6, no. 11, pp. 5656-5675, 2013.

[32] K. Young, C. Wang, L. Y. Wang, and K. Strunz, "Electric vehicle battery technologies," in *Electric vehicle integration into modern power networks*: Springer, 2013, pp. 15-56.

Appendix A. The overall Matlab Simulink model of the E-RSAPHT.